Published at the 23rd IEEE Israel Convention, pp. 44- 48, Tel-Aviv, 2004

APPROXIMATE ANALYSIS OF THE RESONANT LCL DC-DC CONVERTER

Gregory Ivensky, Svetlana Bronstein and Sam Ben-Yaakov

Power Electronics Laboratory
Department of Electrical and Computer Engineering
Ben-Gurion University of the Negev
P. O. Box 653, Beer-Sheva 84105, ISRAEL, Phone: +972-8-646-1561, Fax: +972-8-647-2949
Email: sby@ee.bgu.ac.il, Website: www.ee.bgu.ac.il/~pel

ABSTRACT

An approximate analysis of LCL converters operating above and below resonance is presented. The study based on replacing the rectifier and load by an equivalent parallel resistance, applies the fundamental harmonics method and the assumption that the current through the diodes of the output rectifier has a sinusoidal waveform. Equations obtained for the conduction angle of these diodes (less than π in Discontinuous and equal to π in Continuous Conduction Modes) are used for the developing the output to input voltage ratio as a function of three independent parameters. The theoretical results coincide with good agreement with the experiments.

1. INTRODUCTION

LCL converters have a number of advantages: they can operate in both step up and step down modes, they will accommodate a wide range of output to input voltage ratios with a relatively small frequency deviation, and soft switching could be achieved over the entire operating range [1]-[4]. Approximate analysis of LCL converters operating in Continuous Conduction Mode (CCM) above resonance is described in [4].

The objective of the present study was to develop a simple approximate analysis of LCL converters operating above and below resonance. The focus of attention was devoted to the Discontinuous Conduction Mode (DCM), but the results are applicable to the Continuous Conduction Mode (CCM) as well. The study is based on the equivalent circuit concept in which the rectifier and load are replaced by an equivalent parallel resistance [5], [6], and applies the fundamental harmonics method.

2. ANALYSIS

The LCL resonant inverter topology can be implemented as a full-bridge, half-bridge or half-way type [7], and the output rectifier could be built as a full-wave bridge or as a full-wave center tapped configuration with capacitive output filter. Fig. 1 represents one of the possible realizations of the LCL converter: L_1-C-L_2 is the LCL resonant tank, T is a transformer, $n=n_1:n_2$ is the turns ratio, D_1-D_4 are the diodes of the rectifier, C_f is the output filter capacitance, and R_o is the load resistance. The current and voltage waveforms for the DCM variation are depicted on Fig. 2.

2.1 Main assumptions

The analysis is carried out under the following main assumptions:

a) Switches, diodes, the transformer and all reactive elements are ideal.

b) The current through the diodes D_1 ... D_4 of the output rectifier has a sinusoidal waveform:

$$i_D = I_{D.pk} \sin\left(\frac{\pi}{\lambda}\vartheta\right) \tag{1}$$

where $\vartheta = \omega t$ is the normalized time, counting from the diode turn on instant ϑ_o, t is the real time, ω is the operating frequency, $\lambda \le \pi$ is the conduction angle, $I_{D.pk}$ is the peak value of the diode current. The latter can be expressed as a function of the load current I_o or load voltage V_o:

$$I_{D.pk} = I_o \frac{\pi^2}{2\lambda} = \frac{V_o}{R_o}\frac{\pi^2}{2\lambda} \tag{2}$$

c) The current through the inductor L_2 during the conduction angle λ is changing linearly:

$$i_{L2} = I_{L2o} + \Delta I_{L2}\frac{\vartheta}{\lambda} \tag{3}$$

where I_{L2o} is the initial value of the current i_{L2} and ΔI_{L2} is the increment of the current i_{L2} during the conduction angle λ. This current increment can be expressed as a function of the load voltage referred to the primary nV_o:

$$\Delta I_{L2} = \frac{nV_o\lambda}{\omega L_2} \tag{4}$$

Taking into account (2), we transform (4) to:

$$\Delta I_{L2} = \frac{2I_{D.pk}}{n}\frac{n^2R_o}{\omega L_2}\left(\frac{\lambda}{\pi}\right)^2 \tag{5}$$

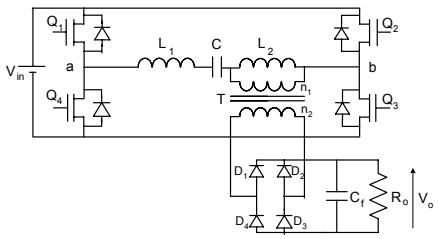

Fig. 1. LCL resonant inverter topology.

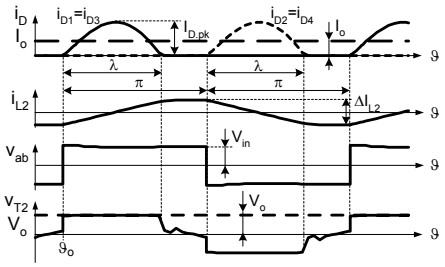

Fig. 2. Currents and voltages waveforms. DCM.

2.2 The diodes' conduction angle

The diodes' conduction angle λ can be obtained from the following equation that is derived by Kirchoff's law:

$$v_{ab} = \omega L_1 \frac{d\left(\frac{i_D}{n} + i_{L2}\right)}{d\vartheta} + \frac{1}{\omega C}\int\left(\frac{i_D}{n} + i_{L2}\right)d\vartheta + V_{Co} + \omega L_2 \frac{di_{L2}}{d\vartheta} \quad (6)$$

where v_{ab} is the instant voltage across the diagonal ab of the inverter bridge (Fig. 1) and V_{Co} is the initial value of the capacitor's C voltage. We consider a time interval where the voltage v_{ab} is constant: $v_{ab}=V_{in}$ (V_{in} is the input voltage) and when identical diodes of the rectifier continue to conduct. In this time interval the voltage across the inductor L_2 is equal to the reflected output voltage:

$$\omega L_2 \frac{di_{L2}}{d\vartheta} = nV_o \quad (7)$$

and the voltage across the inductor L_1 has a constant component proportional to the reflected output voltage:

$$\omega L_1 \frac{di_{L2}}{d\vartheta} = nV_o \frac{L_1}{L_2} \quad (8)$$

Taking into account (7) – (8) we simplify (6) to:

$$V_{in} = \left(1 + \frac{L_1}{L_2}\right)nV_o + \omega L_1 \frac{d\frac{i_D}{n}}{d\vartheta} + \frac{1}{\omega C}\int\left(\frac{i_D}{n} + i_{L2}\right)d\vartheta + V_{Co} \quad (9)$$

Taking the derivative of (9) we find:

$$0 = \omega L_1 \frac{d^2\frac{i_D}{n}}{d\vartheta^2} + \frac{1}{\omega C}\left(\frac{i_D}{n} + i_{L2}\right) \quad (10)$$

Applying (1) and (3) we transform (10):

$$0 = -\frac{I_{D.pk}}{n}\omega L_1\left(\frac{\pi}{\lambda}\right)^2 \sin\left(\frac{\pi}{\lambda}\vartheta\right) + \frac{1}{\omega C}\frac{I_{D.pk}}{n}\sin\left(\frac{\pi}{\lambda}\vartheta\right) + \frac{1}{\omega C}\left(I_{L2o} + \Delta I_{L2}\frac{\vartheta}{\lambda}\right) \quad (11)$$

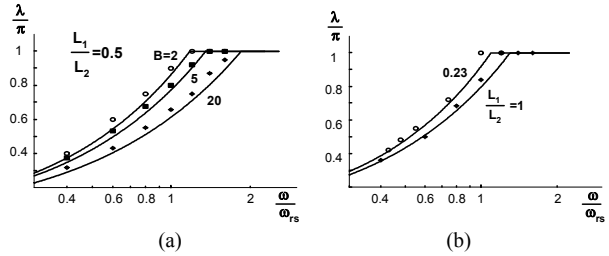

Fig. 3. The ratio λ/π versus normalized operating frequency ω/ω_{ps} for different values B (a) and L_1/L_2 (b) (dots – simulation, solid lines – theoretical prediction).

From which:

$$\left[-\left(\frac{\omega}{\omega_{rs}}\right)^2\left(\frac{\pi}{\lambda}\right)^2 + 1\right]\sin\left(\frac{\pi}{\lambda}\vartheta\right) + \frac{I_{L2o}n}{I_{D.pk}} + \frac{\Delta I_{L2}n}{\pi I_{D.pk}}\frac{\pi}{\lambda}\vartheta = 0 \quad (12)$$

In the last equation:

$$\omega_{rs} = \frac{1}{\sqrt{L_1 C}} \quad (13)$$

is the resonant frequency of the series circuit L_1C.

Applying the assumption:

$$|I_{L2o}| << \frac{I_{D.pk}}{n} \quad (14)$$

and taking into account (5) we obtain from (12) the approximate expression of the conduction angle λ as half sum of two angles:

$$\lambda = 0.5(\lambda_1 + \lambda_2) \quad (15)$$

The angle λ_1 is solution of (12) for the case $\vartheta < 0.1\lambda$, i. e when $\sin\left(\frac{\pi}{\lambda}\vartheta\right) \approx \frac{\pi}{\lambda}\vartheta$:

$$\frac{\lambda_1}{\pi} = \sqrt{-\frac{\pi}{4}\frac{\omega L_2}{n^2 R_o} + \sqrt{\frac{\pi^2}{16}\left(\frac{\omega L_2}{n^2 R_o}\right)^2 + \frac{\pi}{2}\frac{\omega L_2}{n^2 R_o}\left(\frac{\omega}{\omega_{rs}}\right)^2}} \quad (16a)$$

while the angle λ_2 is solution of (12) for the case $\vartheta = 0.5\lambda$:

$$\frac{\lambda_2}{\pi} = \sqrt{-\frac{\pi}{2}\frac{\omega L_2}{n^2 R_o} + \sqrt{\frac{\pi^2}{4}\left(\frac{\omega L_2}{n^2 R_o}\right)^2 + \frac{\pi\omega L_2}{n^2 R_o}\left(\frac{\omega}{\omega_{rs}}\right)^2}} \quad (16b)$$

The value of λ/π as a function of the normalized operating frequency ω/ω_{rs}, calculated by (15), (16a), (16b) for different values of load coefficient $B = n^2 R_o\sqrt{C/L_1}$ and for different inductances ratio L_1/L_2 is depicted on Fig. 3. a,b. The conduction angle λ gets higher for smaller values of B and L_1/L_2. When $\lambda = \pi$, DCM is replaced by CCM. The plots (Fig. 3) also include points that were obtained by PSPICE simulation. The agreement between theoretical prediction and simulation points is good.

2.3 The output to input voltage ratio

To obtain the output to input voltage ratio

$$k_o = \frac{V_o}{V_{in}} \quad (17)$$

we replace the transformer and the rectifier by an equivalent resistance R'_{eq} (Fig. 4a) calculated by energy balance consideration:

$$I_o^2 R_o = \frac{1}{2}I_{(1)pk}^2 \frac{R'_{eq}}{n^2} \quad (18)$$

where $I_{(1)pk}$ is the peak of the fundamental harmonic of the rectifier input current (to simplify the analysis we don't take into account higher harmonics). Under the

second main assumption, the following equation describes the dependence $I_{(1)pk}$ on the load current I_o and the conduction angle λ:

$$I_{(1)pk} = 2I_o \frac{\cos\left(\frac{\lambda}{2}\right)}{1-\left(\frac{\lambda}{\pi}\right)^2} \tag{19}$$

Applying (18) and (19) we define the expression of R'_{eq}:

$$R'_{eq} = \frac{n^2 R_o}{2} \frac{\left[1-\left(\frac{\lambda}{\pi}\right)^2\right]^2}{\cos^2\left(\frac{\lambda}{2}\right)} \tag{20}$$

Note that transition to CCM ($\lambda = \pi$) translates (20) to the known expression [5]:

$$R'_{eq} = \frac{8}{\pi^2} n^2 R_o \tag{21}$$

As a next step of analysis we replace the parallel network $R'_{eq} - L_2$ by the equivalent series network $R''_{eq} - L''_2$ (Fig. 4b) using the following equations:

$$\begin{cases} R''_{eq} = \dfrac{R'_{eq}}{1+\left(\dfrac{R'_{eq}}{\omega L_2}\right)^2} \\ L''_2 = \dfrac{L_2}{1+\left(\dfrac{\omega L_2}{R'_{eq}}\right)^2} \end{cases} \tag{22}$$

Hence, the complete reactance of the inverter is:

$$X_\Sigma = \omega L_1 - \frac{1}{\omega C} + \omega L''_2 \tag{23}$$

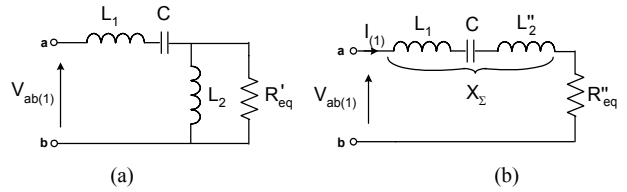

Fig. 4. Series-parallel (a) and series (b) equivalent circuits.

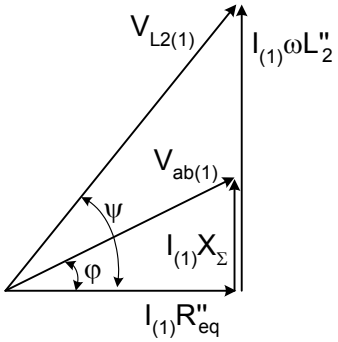

Fig. 5. Vector diagram of the voltages in Fig. 4b.

The ratio between the peaks of the fundamental harmonics of the voltages across the inductor L_2 and across the diagonal ab of the inverter bridge is defined from the vector diagram (Fig. 5):

$$\frac{V_{L2(1)pk}}{V_{ab(1)pk}} = \frac{\cos\varphi}{\cos\psi} = \sqrt{\frac{1+\left(\dfrac{\omega L''_2}{R''_{eq}}\right)^2}{1+\left(\dfrac{X_\Sigma}{R''_{eq}}\right)^2}} \tag{24}$$

where φ is the angle between the vectors $V_{ab(1)pk}$ and $I_{(1)}R''_{eq}$, while ψ is the angle between the vectors $V_{L2(1)pk}$ and $I_{(1)}R''_{eq}$; $I_{(1)}$ is the peak of the fundamental current through the network (Fig.4b).

To obtain the input to output voltage ratio, the peak voltage $V_{ab(1)pk}$ in (24) needs to be expressed as a function of the inverter's input voltage V_{in} while $V_{L2(1)pk}$ in the same equation should be expressed as a function of the reflected output voltage nV_o.

The instant voltage across ab has a square waveform with steps $\pm V_{in}$ (Fig. 2). Therefore, under the first harmonics assumption $V_{ab(1)pk}=4V_{in}/\pi$ is the fundamental harmonics of V_{in}.

The expression $V_{L2(1)pk}$ as a function of nV_o is more complicated because the equation $v_{L2} = \pm nV_o$ is valid only during the rectifier conduction angles $\lambda < \pi$ (Fig. 2). We obtain the expression $V_{L2(1)pk} = \varphi(nV_o)$ using following additional assumptions:

1. The symmetrical axis of the waveform of the inductor L_2 voltage coincides with the middle of the rectifier conduction angle.

2. The waveform of the inductor L_2 voltage coincides with its fundamental harmonic during the time intervals when both diodes of the rectifier are not conducting.

Under these assumptions:

$$V_{L2(1)pk} = nV_o \frac{4\sin\left(\frac{\lambda}{2}\right)}{\lambda + \sin\lambda} \tag{25}$$

Applying (17), (24) and (25) we derive the expression of the output to input voltage ratio as:

$$k_o = \frac{\lambda + \sin\lambda}{n\pi \sin\left(\frac{\lambda}{2}\right)} \sqrt{\frac{1+\left(\dfrac{\omega L''_2}{R''_{eq}}\right)^2}{1+\left(\dfrac{X_\Sigma}{R''_{eq}}\right)^2}} \tag{26}$$

The reflected output to input voltage ratio $nk_o=nV_o/V_{in}$ as a function of the normalized operating frequency ω/ω_r, load coefficient B and inductances ratio L_1/L_2, calculated using the obtained equations, is depicted on Fig. 6, a, b.

3. EXPERIMENTAL

The experimental set up included a half-bridge inverter and a full bridge output rectifier. The inverter was built around a half bridge configuration with two power MOSFETs (IRF840), LCL resonant tank, and planar transformer (200W T250DC-4-24 by Payton, n=3:1). Inductances of the tank were constructed on ETD29 3F3 cores using Litz wire. The rectifier diodes were MUR460. The input voltage was kept constant around 100V. Load resistance varied from 10Ω to 250Ω. Parallel inductance L_2 was 78μH. Series inductance was varied: 16μH, 38.5μH, and 95μH. Operating frequency was varied from 40kHz to 500kHz, covering all operating modes. Maximum power involved in experiment was 70W. It was limited by high hard-switching losses when operating at low frequencies. Experimental voltage ratios nk_o as a function of the load resistance R_o for different frequencies (Fig. 7), and as a function of the operating frequency for different load resistances (Fig. 8, a,b), show good agreement with the theoretical predictions.

4. DISCUSSION AND CONCLUSIONS

An approximate analysis of the resonant LCL converter was carried out, based on the equivalent circuit concept and applying the fundamental harmonics method. The convenient approximate closed formed equations derived for the conduction angle and output to input voltage ratio as a function of three independent normalized parameters (frequency, load resistance and inductances ratio) allow to define the operating regime of the converter for the given circuit parameters and operating frequency and can be used in the design purpose. The analytical results were examined by simulation and experiment and found to be in a good agreement.

Although this study gave focus attention to the DCM, analytical expressions obtained here are applicable to the CCM as well by setting $\lambda=\pi$ in the calculations.

Notwithstanding the fact that some of the expressions developed in this study looks complex, their use is obviously simple once implemented into computer mathematical packages such as MATLAB, Mathematica or MathCad. Hence, the analytical expressions developed in this study could help the designer to study the behavior of a given LCL converter and to optimize the values of the elements per the target specifications.

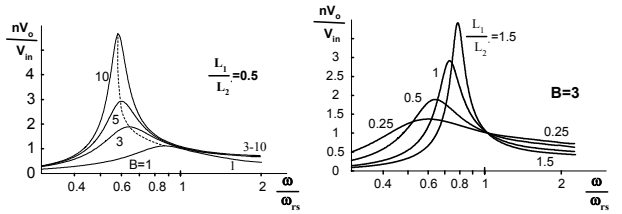

(a) (b)

Fig. 6. Input to output voltage ratio versus normalized operating frequency for different values of B (a) and L_1/L_2 (b).

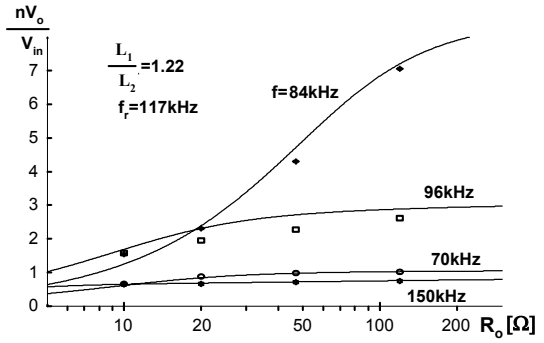

Fig. 7. Input to output voltage ratio as a function of the load resistance for different operation frequencies (dots – experiment, solid line – theoretical prediction).

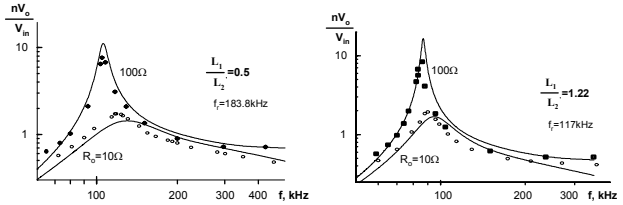

(a) (b)

Fig. 8. Input to output voltage ratio as a function of the operating frequency for different load resistances (dots – experiment, solid line – theoretical prediction).

ACKNOWLEDGMENT

This research was supported by THE ISRAEL SCIENCE FOUNDATION (grant No. 113/02) and by the Paul Ivanier Center for Robotics and Production management.

5. REFERENCES

[1] J. F. Lazar and R. Martinelli, "Steady-state analysis of LLC series resonant converter," *IEEE APEC'2001 Record*, pp. 728-735.

[2] H. Jiang, G. Maggetto, and P. Lataire, "Steady-state analysis of the series resonant DC-DC converter in conjunction with loosely coupled transformer – above resonance operation," *IEEE Trans. Power Electronics*, vol. 14, no. 3, May 1999, pp. 469-480.

[3] Bo Yang and F. C. Lee, "LLC resonant converter for front end DC/DC conversion," *IEEE APEC'2002 Record*, pp. 1108-1112

[4] A. K. S. Bhat, "Analysis and design of LCL-type series resonant converter," *IEEE Trans. Industrial Electronics*, vol. 41, no. 1, Feb. 1994, pp. 118-124.

[5] R. L. Steigerwald, "A comparison of half-bridge resonant converter topologies," *IEEE Trans. Power Electronics*, vol. 3, no. 2, pp. 174-182, Apr. 1988.

[6] G. Ivensky, A. Kats, and S. Ben-Yaakov, "An RC load model of parallel and series-parallel resonant converters with capacitive output filter," *IEEE Trans. Power Electronics*, vol. 14, no. 3, pp. 515-521, May 1999.

[7] M. K. Kazimerczuk and D. Czarkowski, "*Resonant power converters*," John Wiley & Sons, Inc., 1995.